X-ray scattering from epitaxial GaSb/InAs thin films below and above the critical thickness

2002 J. Phys.: Condens. Matter 14 7101

(http://iopscience.iop.org/0953-8984/14/30/302)

INSTITUTE OF PHYSICS PUBLISHING JOURNAL OF PHYSICS: CONDENSED MATTER

J. Phys.: Condens. Matter **14** (2002) 7101–7121 PII: S0953-8984(02)27638-9

X-ray scattering from epitaxial GaSb/InAs thin films below and above the critical thickness

A Yu Babkevich[1], R A Cowley[1], N J Mason[1], S Sandiford[1] and A Stunault[2]

[1] Clarendon Laboratory, Oxford University, Parks Road, Oxford OX1 3PU, UK
[2] XMaS, ESRF, BP220, 38043 Grenoble Cedex, France

Received 6 August 2001, in final form 18 February 2002
Published 17 July 2002
Online at stacks.iop.org/JPhysCM/14/7101

Abstract

The structure of layers of GaSb grown on InAs substrates has been investigated by means of high-resolution x-ray diffraction. The samples were grown in Oxford using the metal–organic vapour phase epitaxy facility to produce high-quality single-crystal layers with thicknesses between 60 and 3000 Å. The x-ray scattering experiments were performed with a Philips MRD diffractometer in Oxford and with the XMaS facility at the ESRF. The results show that the scattering for layers with a thickness below $T_c' \sim 1250$ Å is different from the scattering for those with larger thicknesses. The scattering from the thinner layers shows that the in-plane lattice constant of the GaSb is very close to that of the InAs substrate and that the strain does not vary through the film, while the measured diffuse scattering is in good agreement with calculations of the scattering from isolated 60° dislocations. The thicker layers show no diffuse scattering but single-Gaussian Bragg peaks and the scattering is that expected from a mosaic layer with a large concentration of 60° dislocations. Analysis of the peak parameters shows that the average in-plane lattice constant is intermediate between those of bulk GaSb and bulk InAs and that there is a changing strain through the film. The critical thickness T_c for GaSb on InAs is calculated as about 204 Å. We argue that between 204 and 1250 Å there are only a few dislocations, but thicker films are relaxed by spontaneous creation of a dislocation network. The results demonstrate the power of high-resolution x-ray scattering for studying non-destructively the structures of thin films containing dislocations, and show that there is a marked change in the scattering for layers above the critical thicknesses T_c and T_c'.

(Some figures in this article are in colour only in the electronic version)

1. Introduction

Understanding of the relaxation process in lattice-mismatched epitaxial layers is important for both fundamental and technological reasons. The practical implications of this understanding include the ability to predict the conditions needed for high-quality pseudomorphic crystal growth and the precision of lattice matching in structures where no strain can be tolerated, such as semiconductor lasers and photovoltaic devices. One application is for optical devices, where alternating layers of material are used as a long-wavelength infra-red detectors while others are for infra-red quantum cascade lasers or resonant tunnelling. The optical and electrical properties are very dependent on the presence or absence of dislocations in the materials and so a detailed understanding of the generation and control of the dislocations is of crucial importance to the use of these materials in solid-state electronics [1, 2]. Dislocations may be introduced into growing crystals for a number of reasons and it is important to distinguish between them when looking at relaxation. Firstly the quality of the substrate both in the bulk and the surface is important. No substrate is free of surface imperfections or bulk defects and both of these can introduce dislocations in the epitaxial layer. In this study we are more concerned with the dislocations that are introduced because they reduce the strain in an epitaxial layer mismatched in lattice constant from the substrate.

It is generally believed that below a certain thickness an overlayer grows in coherence with the substrate and that no dislocations are produced at the interface. When a layer exceeds the *critical thickness*, dislocations are generated and the overlayer has an in-plane lattice constant different from that of the substrate and approaches the lattice constant of the bulk. A knowledge of the critical thickness is then vital and in this work we have used high-resolution x-ray diffraction to determine it for the GaSb layers grown on InAs substrates.

Comparison of the misfit dislocation structures observed by electron microscopy for a variety of heteroepitaxial systems shows that the dislocations are generally of the 60° type when the misfit is small, are of mixed 60° and 90° types for intermediate degrees of misfit and are predominantly of the Lomer 90° type for very large degrees of misfit. Because the GaSb/InAs interface has a low mismatch (about 0.6%), it 60° dislocations are anticipated to dominate in this system. The 60° dislocations have their Burgers vector at an angle of 45° to the plane of the interface and 60° to the dislocation line. The dislocations move by slip along crystallographic planes which contain both their Burgers vector and a dislocation line, i.e. the (111) plane. The (111) planes are the easy-slip planes in GaSb and the dislocations glide through the GaSb epilayer and reach the surface. Such a propagation of dislocations from the interface through the epilayer is called threading and it causes a degradation of the optical and structural properties of the epilayers. We are unaware of any experimental results for the strain relaxation of GaSb on InAs substrates. An x-ray diffraction study by Bennett [3] showed that an MBE-grown InAs layer on a GaSb substrate remains coherently strained for thicknesses up to 2000 Å but no details were given about the dislocation structure. In this paper we describe the results of an x-ray diffraction study of a series of GaSb epilayers of different thickness grown on an InAs substrate and interpret the scattering in terms of the changing dislocation structure with the thickness of the GaSb layers.

Our x-ray scattering measurements have used high-resolution techniques and high-intensity x-ray sources to determine the detailed structure of the layers. Although these techniques have been used previously for other systems we believe that this is the first time that they have been applied systematically to layers with thicknesses above and below the critical thickness and hence we clearly demonstrate the change in the scattering and structure on passing through the critical thickness. We have studied the scattering in detail around several Bragg reflections. This enables us to identify the origin of diffuse scattering with

Table 1. Thickness of GaSb layers determined by different methods.

Sample	Growth time (s)	Optics (Å)	Fringes (Å)	Bragg (002) (Å)	Extrapolation (Å)	Thickness (Å)
3852	75	—	63(4)	—	77(8)	67(5)
3468	300	412(50)	515(30)	556(20)	566(20)	543(20)
3841	1200	1085	1105(50)	1060(30)	1104(30)	1085(20)
3885	1500	—	—	1202(50)	1575(50)	1370(100)
3873	1800	2687(200)	—	1755(50)	3778(80)	2700(300)
3863	2400	2975(200)	—	2126(40)	4533(100)	3000(300)
3454	3000	—	—	—	720(200)	720(200)

much more confidence than if data are only available around one Bragg reflection or only from reflectivity measurements. Our results suggest that there are two thicknesses at which the behaviour of the diffuse scattering changes. For layer thicknesses above the theoretical critical thickness of 204 Å but below about 1250 Å, we show that the diffuse scattering is characteristic of crystals with a very low density of isolated dislocations. The scattering shows a sharp Bragg peak, diffuse scattering, Pendellösung fringes and the lattice parameter in the plane of the layer is close to that of the InAs substrate. The scattering drastically changes at thicknesses above about 1250 Å and the thicker layers have a structure consistent with mosaic crystals with a large dislocation density [4] and a lattice parameter that steadily approaches the bulk GaSb parameter as the thickness increases. The reasons for this behaviour are discussed in section 4.

2. Experiments

Six layers with different thicknesses of GaSb were grown on the (001) plane of single-crystal InAs substrates at 520 °C in the MOCVD growth reactor at the Clarendon Laboratory, Oxford [5]. The serial numbers of the samples and the growth times are listed in table 1. The precursors used were trimethylgallium and antimony and are incompletely pyrolysed at the growth temperature used. This has the effect that when small changes are made in the growth temperature, large changes in the growth rate can occur. The MOVPE reactor has *in situ* monitoring of the growth by optical reflection. This enables an estimate of the thickness of the layers to be made provided that the layer is optically thick (i.e. the interferogram shows a turning point) and for the materials discussed here that thickness is above 330 Å. The optical thicknesses listed in table 1 are based on the *in situ* monitoring. For the purpose of comparison a layer of InAs was grown on a GaSb substrate under similar experimental conditions and its parameters are also listed in table 1.

The x-ray scattering measurements were performed at the XMaS beamline (BM28) at the ESRF with the incident beam having a wavelength $\lambda = 1.127\,16$ Å and with a triple-crystal Philips MRD high-resolution x-ray diffractometer in Oxford with an incident wavelength $\lambda_{K\alpha 1} = 1.540\,56$ Å (Cu radiation). The scattering vector $\boldsymbol{q}$ was varied parallel and normal to the film surface through the centre of the GaSb and InAs substrate peaks. It is defined by two components, $\boldsymbol{q}_x$ and $\boldsymbol{q}_z$, where $\boldsymbol{q}_z$ is the component parallel to the growth direction [001] and $\boldsymbol{q}_x$ is the component along the perpendicular [110] direction. Scans in which $\boldsymbol{q}_x$ is varied while $\boldsymbol{q}_z$ is fixed are described as transverse scans, while those in which $\boldsymbol{q}_z$ is varied are called longitudinal scans. For convenience, Bragg reflections will usually be given by conventional triple Miller indices $(H\,K\,L)$ where each of the indices h_i is related to the components of $\boldsymbol{q}$ and to the lattice parameters a_i as $h_i = q_i(\frac{2\pi}{a_i})^{-1}$ rather than by $\boldsymbol{q}$-vector components, where

$q_i = |\boldsymbol{q}_i|$. The wavevector resolution in the scattering plane was determined from the width of the substrate peaks and was typically better than 6.6×10^{-4} Å^{-1}, while that perpendicular to the plane was 3.6×10^{-2} Å^{-1}.

The scattering was measured near the (002), (004), (006) and (115) Bragg reflections of both the layer and the substrate. Reflectivity measurements did not provide useful data because the contrast between GaSb and InAs is too small. Another advantage of studying the scattering around the Bragg reflections from thin layers is that the scattering is only a small fraction of the incident beam and kinematical theory can be used to interpret the results.

2.1. Longitudinal scans

Measurements of the x-ray intensity when the scattering vector is varied longitudinally, parallel to the [001] (growth) direction and through the Bragg reflections of the layers, provide information about:

(i) the lattice parameter of the layer in the growth direction,
(ii) the thickness of the layer,
(iii) the variation of the strain in the growth direction and
(iv) the roughness of the top and bottom surfaces of the layer.

We now comment on how the different parts of this information can be obtained from the observed scattering.

The scattering from an ideal layer consisting of $N + 1$ planes with an inter-planar spacing, a, is given by

$$I(q_z) = |F(q_z)|^2 \frac{\sin^2(q_z a N/2)}{\sin^2(q_z a/2)} \tag{1}$$

where $F(q_z)$ is the structure factor of the planes. The intensity has strong Bragg peaks for $q_z = |\boldsymbol{q}_z| = \frac{2\pi}{a}L$, where L is a Miller index, and subsidiary satellite peaks (so called Pendellösung fringes) for $q_z = \frac{2\pi L}{aN}(N \pm (n + \frac{1}{2}))$, where $n = 1, 2, \ldots$ is a satellite index. The positions of the strong Bragg peaks provide information about the average lattice parameter, a, and hence the average uniform strain while the spacing of the satellite peaks gives a measure of the thickness of the layer $T = Na$. The thickness T can also be obtained from the full width at half-maximum (FWHM) of the strong Bragg peaks, Δq_z, and it follows from equation (1) that $T = 5.566\,24/\Delta q_z$. Hence, if T increases, the width of the Bragg peaks and the spacing of the satellite (Pendellösung) peaks decreases. This analysis is consistent only if the width of the strong Bragg peaks is independent of the Bragg reflection and hence of L. In our experiments, particularly for the thicker (>1000 Å) layers, the widths of the Bragg peaks increase with L and the Pendellösung fringes could not be observed. This arises from the strain of the layer and shows that obtaining the thickness of a layer from the longitudinal scans requires care.

The analysis and separation of size effects from random strain effects has been discussed for powder samples by Langford [6, 7]. The line-shape of powder Bragg peaks is believed to be determined by Lorentzian and Gaussian components both contributing to a composite Voigt line-shape of Bragg peaks. Size and strain effects can be separated by using the wavevector dependence of the widths.

The case of thin layers grown on a substrate is more complicated. Firstly, there may be a randomness in the strain due to imperfections and dislocations and, secondly, a varying strain due to a monotonic lattice parameter variation from top to bottom of the layer if the lattice parameter is that of the substrate at the bottom and that of the bulk layer material at the top of the layer. We shall discuss the effect on the scattering of both of these types of variation in the strain.

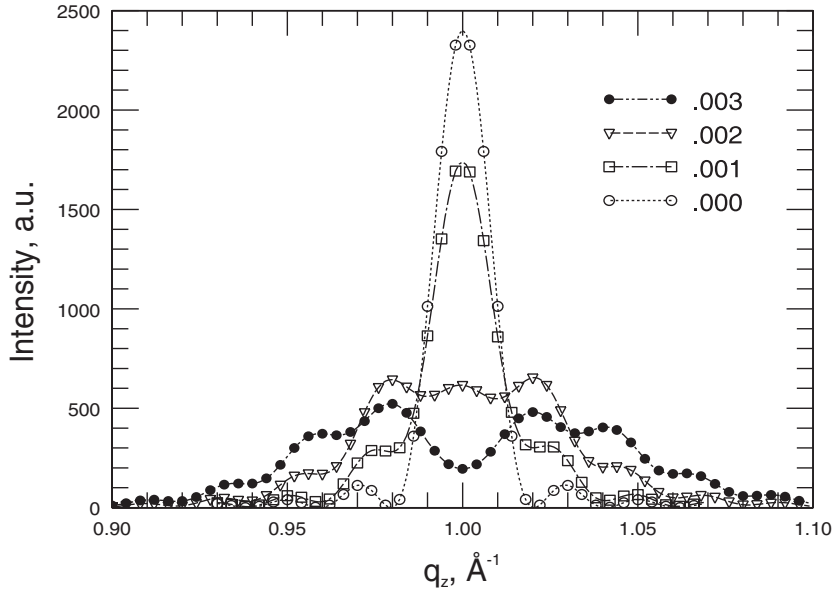

Figure 1. The scattering from a strained layer of 99 atomic planes calculated for different values of the non-linear strain parameter γ.

X-ray diffraction from crystals with a linear lattice parameter variation has been considered in detail in [8–10]. It was shown that the widths of the Bragg peaks have a complex variation with the thickness. The variation of the width with the thickness is vital for determining the thicknesses of the films and therefore we have investigated the effect of a linear lattice parameter variation on the x-ray scattering in more detail using a simple computer simulation. The aim of the calculation was to find how the FWHM depends on the thickness and Miller indices L of the Bragg reflections. The results of our kinematical theory are qualitatively consistent with those of Kolpakov *et al* [8].

The scattering from a thin layer has been calculated when there is a linear lattice parameter variation throughout the layer so that $a = \overline{a} + \gamma l$ and the plane index l runs from $-(N-1)/2$ to $(N-1)/2$, where $\overline{a}$ is an average inter-planar spacing determined from the measured lattice constant of the film. The total change in the strain through the layer is at most the difference between the bulk material lattice parameter of the substrate and the layer and within our model is $N\gamma$. The scattering for wavevectors close to the first Bragg reflection, (002) GaSb, was calculated for layers with 49 and 99 planes and for several values of γ. Some of the results are shown in figure 1. As γ increases the Pendellösung fringes cease to be visible while the width of the strong Bragg peak increases slightly. A further increase in γ leads to structure in the main Bragg peak with subsidiary peaks at the first minima of the scattering from a perfect layer (figure 1; $\gamma = 0.001$ and 0.002), and then to a minimum in the scattering at the centre of the Bragg reflection (figure 1; $\gamma = 0.003$). The results of the calculations were fitted to a Gaussian to give the FWHM, of intensity FWHM, Δq_z, and all the calculations for different thicknesses showed that the results for Δq_z could be described by a universal scaling form if $N\,\Delta q_z$ was plotted as a function of $Y = \gamma L N^2$. This scaling function is shown in figure 2. The widths increase with increasing index of the Bragg reflection, L, and for large Y the increase is a nearly linear function of Y. As reported in [8] and shown in figure 1, this faster increase of the width of the Bragg peaks occurs at higher thicknesses or, strictly speaking, at higher Y-values

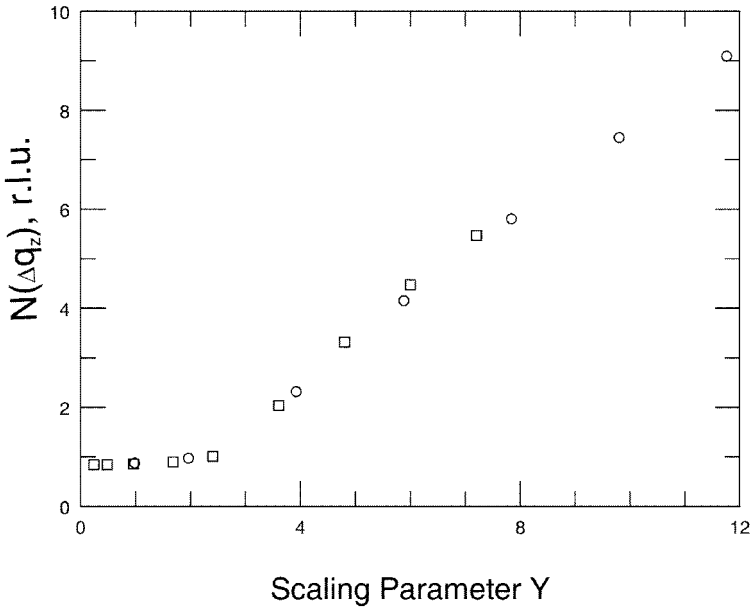

Figure 2. The scaling function for the width of the Bragg peak as a function of the parameter $Y = \gamma L N^2$ described in the text.

and is associated with a complex line-shape for the Bragg reflections. We have not observed a complex shape in our experiments, most probably because the variation of the strain is not constant through the layer. For this reason we believe that fitting of the calculated profile to a Gaussian provides a reasonable measure of the widths of the Bragg reflections.

Similar but exponentially varying strain has been considered by Lin *et al* [11] but the details of the x-ray scattering near the Bragg peaks were not given. Fewster [12, 13] used a dynamical simulation of diffraction profiles assuming that the lattice parameter changes linearly from that of a bulk at the layer surface to some intermediate value at the top of a defect region confined to the interface and exponentially down to the interface. Unfortunately the details of the Bragg scattering expected from the model were not discussed.

Our other calculation assumes a Gaussian distribution of the strain throughout a thick (10^4 atomic planes) layer such that there is a variance $\sigma = \delta a$ in the lattice constant a determined by the parameter δ. The Bragg peaks were then accurately described by Lorentzian profiles with the FWHM given by $\Delta q_z^s = \delta q_z^2$ as shown in figure 3. Comparison of figures 2 and 3(c) shows that the dependence of the FWHM on the wavevector q_z for a random strain is different from that for a linearly varying strain. In the former case for large q_z the FWHM is proportional to q_z, whereas in the latter case it is quadratic. For a thin layer the width due to the thickness should also be included. As discussed above, the FWHM due to the thickness is given by $\Delta q_z^T = 5.566\,24/T$ and the line-shape of the main (Bragg) peak is approximately Gaussian. In general the broadening from the strain in thin layers can be distinguished from that of the thickness because the latter is independent of the Bragg reflection, whereas the former increases with the wavevector of the Bragg reflection and in that respect the procedure is similar that proposed by Langford [6, 7] for powder samples. These results show that the thickness can only be obtained correctly by extrapolating the width of the Bragg reflections to $q_z = 0$ and that the variation of the FWHM with wavevector, q_z, provides information about the nature of the strain variation in the layer.

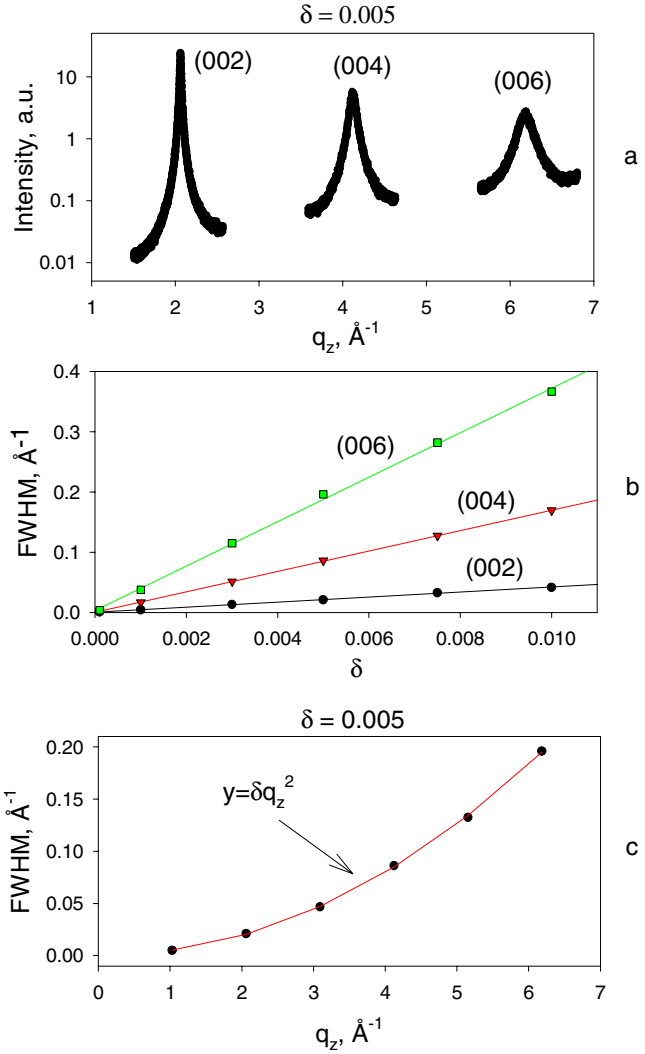

Figure 3. The x-ray scattering from crystal with a random (Gaussian) strain. Parameter δ is related to the variance σ of the lattice constant a as $\sigma = \delta a$: (a) the intensity along q_z ($q_x = 0, \delta = 0.005$); (b) the variation of FWHM of the (002), (004) and (006) reflections as a function of δ; (c) the variation of the FWHM versus q_z. The FWHM can be approximated by the line $y = \delta q_z^2$.

2.2. Transverse scans

The transverse scans, i.e. scans with the scattering vector varying perpendicular to the growth direction through the Bragg reflections, provide information about the deformations of the planes parallel to the growth direction. If the planes are flat and undistorted, the scattering is a Bragg-like delta function. In practice, as illustrated in section 3, the scattering is usually more complicated: the peaks are frequently broad in q_x and there may also be subsidiary peaks centred at non-zero values of q_x. These effects may arise in two ways. Firstly, the planes may be distorted away from the ideal position and the distortion extend only a finite distance, the correlation length. Subsidiary peaks then arise if the distortions are periodic deformations of

the planes such as may be caused by regular arrays of misfit dislocations [13, 14]. Periodic distortions with a finite correlation length give the same broadening and positions in wavevector, q_x, around each Bragg reflection, L. The relative intensities of the Bragg peaks and of any subsidiary structure may vary because the distortions of the planes give rise to a Debye–Waller type of effect on the Bragg reflections. The corresponding decrease in the relative intensity of the Bragg peaks with increasing L then gives a measure of the mean square displacement, $\langle U_z^2 \rangle$. In addition there may be L-dependent terms in the scattering cross section for the subsidiary peaks.

Secondly, if the planes are tilted, any broadening of the peaks in q_x will increase as L increases. These tilts may arise, for example, if the surface of the substrate is miscut from the atomic plane by an angle φ when, if a_s and a_f are the lattice a-spacings of the substrate and the film respectively, the tilt of the film from the substrate is $(1 - a_f/a_s)\varphi$, but more usually tilts occur if there is a network of 60° dislocations. Usually both tilting and finite-size effects are present because if there are tilts each tilted region must be of finite extent if the layer is to remain in contact with the substrate. The tilting effect and the finite coherence length can be distinguished experimentally for simple distributions of the tilts by comparing the scattering for different Bragg reflections, L, and by reciprocal-space mapping of asymmetrical reflections.

3. Experimental results

3.1. The layer thickness

The thicknesses of the layers were determined initially from the broadening of the Bragg peaks observed in longitudinal scans through the Bragg reflections of the GaSb layer and the InAs substrate. The scattering is shown for two samples in figure 4 and the peaks were fitted to a Pearson VII function to obtain the position and width, Δq_z. The fitting function shape parameter showed that the Bragg peaks are approximately Gaussian. The instrumental resolution function, IRF, was obtained from the Bragg reflections of the InAs substrate. The substrate peaks are also Gaussian in shape and so the observed peak width Δq_z is given by

$$\Delta q_z^2 = (\Delta q_z^L)^2 + \Delta_{IR}^2 \tag{2}$$

where Δq_z^L is the broadening due to the finite thickness of a layer and any sample imperfections and Δ_{IR} is the broadening due to the instrumental resolution. As explained in section 2.1, the thickness of the layer can be obtained from the extrapolation of the Δq_z^L to $q_z = 0$. This extrapolation was performed by assuming $(\Delta q_z^L)^2 = (\Delta q_z^T)^2 + (\Delta q_z^s)^2$ where Δq_z^T is the contribution of the thickness and Δq_z^s is the contribution from the strain and is assumed to be proportional to the wavevector q_z if the strain varies uniformly throughout the layer. The simulations discussed above show that this is reasonable for large strains but will tend to underestimate Δq_z^T and so the method will overestimate the layer thickness if there is a wavevector dependence of the widths.

A lower limit on the layer thickness can be obtained from the width Δq_z^L as $T = 5.566\,24/\Delta q_z^L$ for the Bragg reflection with the smallest index, L, i.e. from the (002) reflection. This width may be larger than the width due to the thickness because of a changing strain and so the resulting calculated thickness is lower than the actual thickness. The separation of the Pendellösung fringes, if they can be observed, gives another measure of the thickness of the layers. Finally, as discussed in section 2, the optical reflectivity obtained during the growth process allows a further estimate of the thickness of the layers provided that the growth rate is uniform. We have used the x-ray scattering data for sample 3841 to calibrate the optical reflectivity measurements. The results from these different methods of estimating the thickness of the samples are listed in table 1.

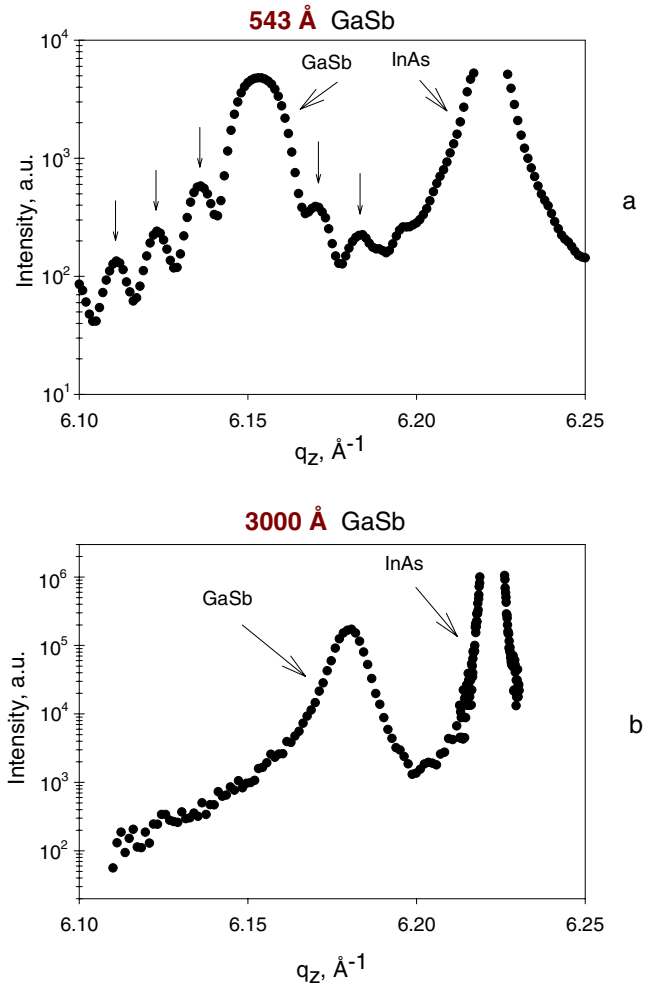

Figure 4. X-ray scattering observed from thin (a) and thick (b) layers of GaSb grown on InAs when the wavevector transfer varied longitudinally through the (006) Bragg reflections. The arrows in (a) show the position of the Pendellösung fringes.

The scattering from the thinner samples, as illustrated in figure 4(a), shows peaks from the GaSb and the InAs substrate and a number of Pendellösung fringes from the finite thickness of the GaSb layers. In the case of the thinnest layer, 3852, the width of the (002) GaSb peak is so large that it strongly overlaps with the much more intense InAs substrate peak and so it was not possible to determine its width reliably. Likewise it is difficult to determine the widths of the (004) and (006) reflections and so the most reliable measure of the thickness comes from the separation of the Pendellösung peaks. The other two thin samples, 3468 and 3841, also showed fringes and these again provided a reliable measure of the thickness. The widths of the Bragg peaks were, within error, independent of the index of the Bragg reflection L for the (002), (004) and (115) Bragg reflections of the 3468 layer, figure 5(a). For these thin layers there is also agreement between the thicknesses deduced from the (002) reflection and from the extrapolation method as listed in table 1.

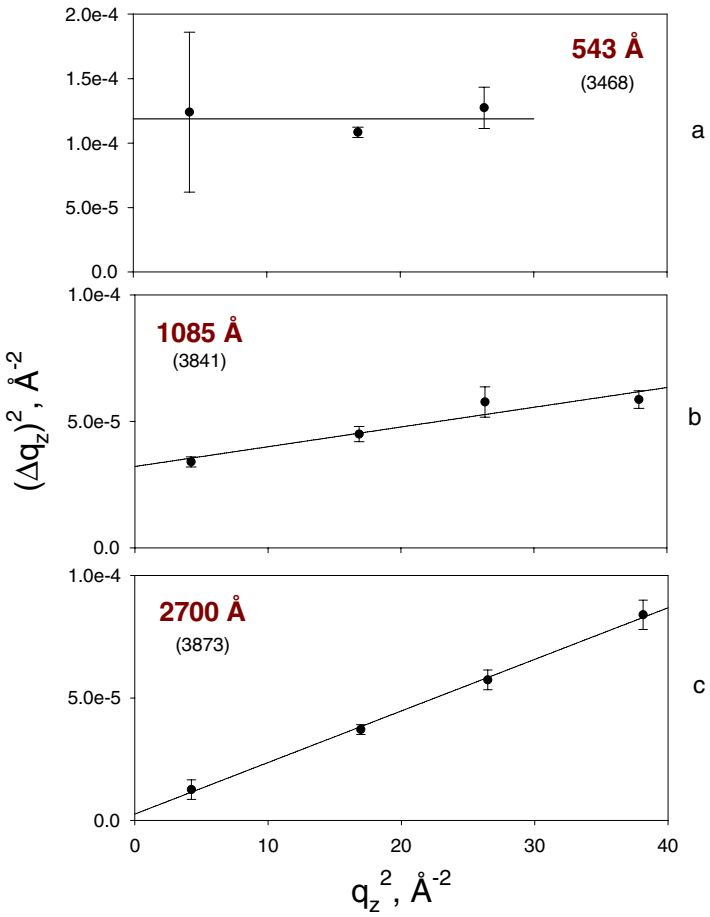

Figure 5. The FWHM of the GaSb Bragg peaks in the q_z-direction as a function of q_z^2 for three film thicknesses.

The scattering from the three thicker layers shows a different behaviour, figure 4(b). The Pendellösung fringes are not observed, indicating either that there is a varying strain through the layers or that there is roughening of the surface of the layer or, most probably, that both effects are present. The widths of the Bragg reflections steadily increase with increasing L showing that the layer is strained. As a consequence, there is now a significant difference between the estimates of the thickness obtained from the extrapolation method and from the (002) reflection, table 1. In the case of layer 3885 the difference between these various techniques is not large and the thickness is obtained with reasonable accuracy. The situation is more difficult for the two thickest samples for which the difference is large. Figures 5(b), (c) show that the width of the Bragg peaks increases approximately linearly with the wavevector q_z, and so the dominant component of the strain is not random but varies linearly through the layer. Unfortunately the x-ray methods then give very different estimates for the thicknesses of these layers and the best estimates of the thickness are from the optical reflectivity measurements. The difficulty with the x-ray measurements is that it is only possible to obtain measurements of the widths for a few Bragg reflections and the extrapolation to $q_z = 0$ cannot be made unambiguously. A direct way out of this problem would be to measure the layer thickness using x-ray reflectivity

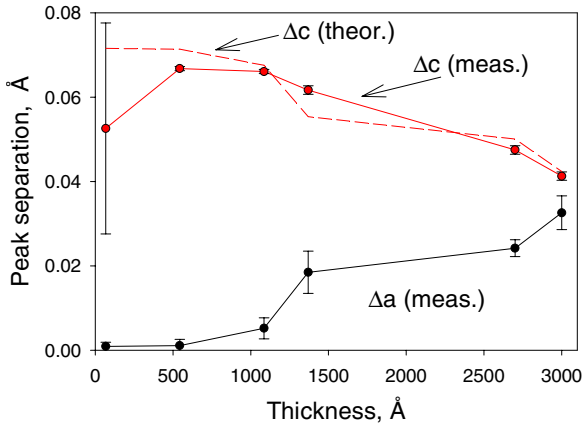

Figure 6. The differences between the lattice parameters a and c of the layers and the substrate. The dotted curve shows a calculation of c from the change in a and elasticity theory.

techniques, but for GaSb and InAs the electron density contrast is negligible and unambiguous results cannot be obtained for the reflectivity.

3.2. Lattice parameters and strain

Bulk samples of GaSb and InAs have a cubic crystal structure with lattice parameters $a_L = a_{\mathrm{GaSb}} = 6.09593$ Å and $a_S = a_{\mathrm{InAs}} = 6.0583$ Å. The lattice mismatch is given by

$$f_m = \frac{a_S - a_L}{a_L} \tag{3}$$

where $f_m = -0.62\%$. When GaSb is grown on InAs it is initially compressed, so the in-plane lattice parameter of the layer, a_L, is contracted to become the same as that of the InAs substrate while the lattice parameter in the growth direction, c_L, is expanded. As the layer becomes thicker it becomes energetically favourable for the strain in the GaSb to be relaxed by the introduction of misfit dislocations and the average lattice constants to relax towards those of bulk GaSb. The lattice parameters of both the layer and the substrate can be obtained from the mean positions of the Bragg reflections. The (002), (004), (006) and (115) reflections were measured and the results fitted as described above to obtain the positions. The systematic errors were minimized by considering only the differences between the positions of the InAs reflections and the similar GaSb reflections. The results for the differences between the lattice parameters of the layer and those of the substrate, $\Delta a = a_L - a_S$ and $\Delta c = c_L - c_S$, are shown in figure 6 as a function of the thickness. The results for c_L for the thinnest layer are very uncertain because the peaks are very broad and of low intensity compared with the InAs peaks, so their positions could not be accurately determined. The results show that for the layers with a thickness of <1000 Å the in-plane lattice constant of the layer, a_L, is, within the error 0.02%, the same as that of the substrate. As the layer thickness increases above 1000 Å the in-plane lattice constants of the layer and substrate differ significantly. The lattice parameter difference rises rapidly, so the misfit is about $f_m/2$ and then steadily increases with further increase in the thickness. The dotted curve in figure 6 gives Δc calculated from the observed Δa by using elasticity theory. The results agree very reasonably with the measurements of Δc.

As discussed above, the change in the width of the Bragg reflections with L is due to the variation of the strain in the layers. Figure 5(a) shows that for the thin layers there

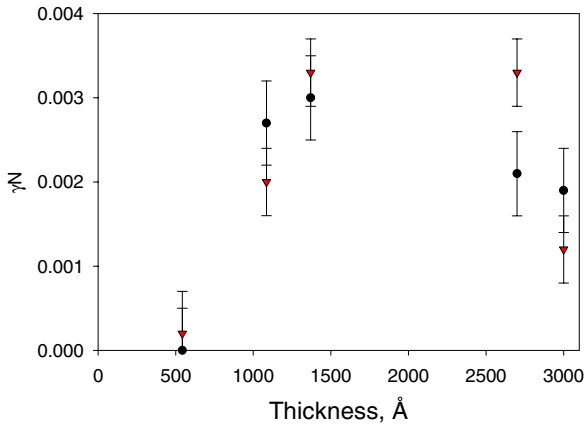

Figure 7. The thickness dependence of the change in strain through the layer. The circular points (●) are deduced from the widths of the Bragg reflections, figure 5, and the triangular points (▼) from the lattice parameters as described in the text.

is little variation in the widths of the Bragg reflections and so the lattice parameter is reasonably constant throughout the thickness of the layer. This is consistent with the layers being epitaxially matched to the substrate with very few dislocations. For the thicker films, figures 5(b), (c), the Bragg peaks have a width that increases with increasing wavevector transfer. The widths of the Bragg reflections and the scaling curve shown in figure 2 enable the difference in strain between the top and bottom of the layer to be calculated and the results are shown in figure 7. The maximum possible difference in strain between the top and bottom of the layer is given by the difference in the lattice parameter c of GaSb between the cases where the in-plane parameter is that of the substrate and that of bulk GaSb. A simple but more refined model is obtained by assuming that the mean lattice parameter of the layer is as given in figure 6 and that the difference between top and bottom is twice the difference between the mean and the closest of either the two lattice parameters described above. The results of this model for the difference in the strain are shown in figure 7 and the very reasonable comparison between the measurements from the Bragg peak widths and the simple model provides good evidence for our explanation of the width of the Bragg reflections as arising from the linear variation in the strain across the layer.

4. Transverse scans

The scattered intensity observed when the wavevector transfer is scanned through the Bragg reflections transversely by varying the q_x-component is shown in figure 8 for the Bragg reflection (004) and in figure 9 for (006). The shape of the scattered intensity varies markedly with the layer thickness. For the three thickest samples the profile is a broadened single peak as illustrated for layer 3863 in figures 8 and 9. For the thinner samples the profiles are more complex and consist of two or more components. Surprisingly, the results for the scattering are qualitatively similar when the layers are rotated so that q_x is along the $[1\bar{1}0]$ direction.

The profile of the scattering from the thinnest layer, 3852, near the (002) Bragg reflection can be described by two components: a sharp component with a FWHM of 0.000 26(1) Å^{-1} and a broad component with a width of 0.0006(2) Å^{-1}. Near the (004) and (006) reflections the scattering is complex as shown in figures 8(a) and 9(a). Near the (004) Bragg reflection,

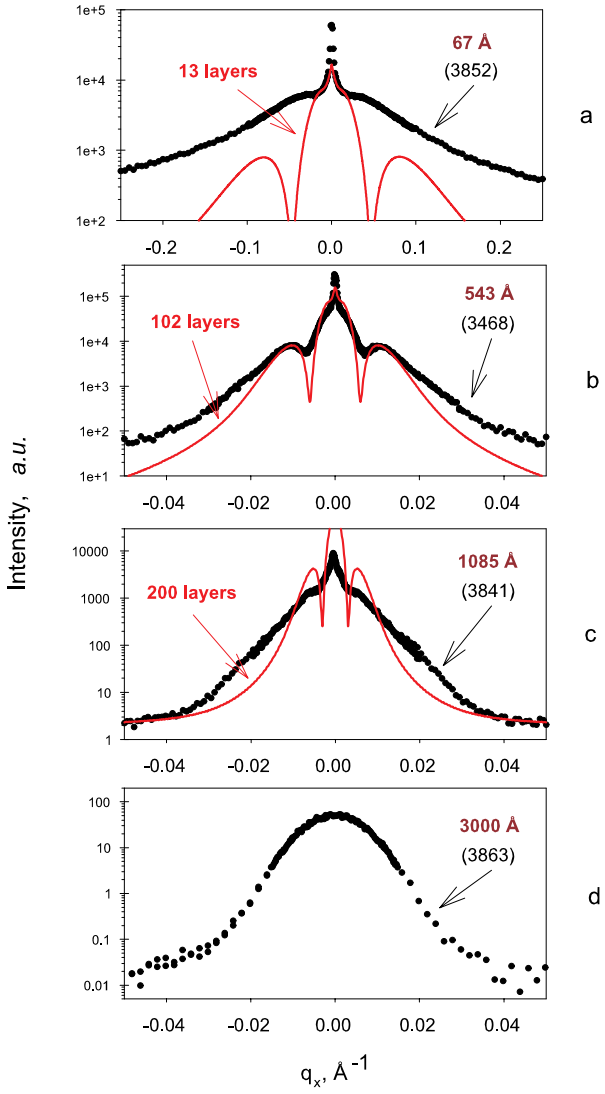

Figure 8. The intensity observed when the wavevector is scanned transversely (q_z = constant) through the (004) GaSb peak for several different film thicknesses. The solid curves show the scattering from an isolated 60° dislocation scaled to the diffuse scattering.

figure 8(a), the narrow component has a FWHM of 0.000 50(1) Å^{-1} and two broad satellite peaks at ±0.030(1) Å^{-1} have a width of 0.106(20) Å^{-1}. The scattering observed near the (006) Bragg reflection, figure 9(a), shows a narrow central peak with a FWHM of 0.000 52(1) Å^{-1} and two side peaks centred at ±0.06(1) Å^{-1} with a width of 0.18(2) Å^{-1}. The sharp component and its width show that the atomic planes are on average flat over large distances of about 25 000 Å. The other components arise from fluctuations in the positions of the atoms from the average planes. Since the width of this scattering increases with L, the fluctuations must arise from localized tilts of the planes.

The scattering profiles from the layer 3468 are more complex. The profile near (002) can be analysed as two components: the sharp component has a width of 0.0005(1) Å^{-1} while the

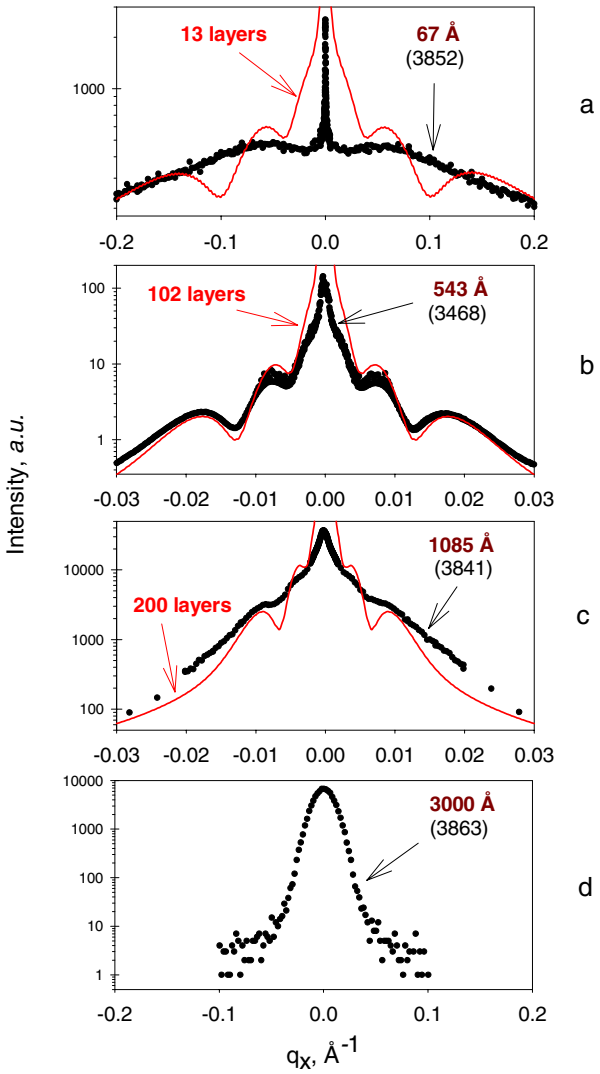

Figure 9. The intensity observed when the wavevector is scanned transversely (q_z = constant) through the (006) GaSb peak for several different film thicknesses. Solid curves show intensities calculated from the theory [4] for 60° misfit dislocations.

broad component has a width of 0.0087(4) Å^{-1}. Near the (004) Bragg reflection the results show a narrow component with a width of 0.0007(1) Å^{-1}, a broad component with a width of 0.005 35(7) Å^{-1} and two broad satellite peaks at ±0.010(1) Å^{-1} with width of 0.006(2) Å^{-1}. The scattering near the (006) Bragg reflection is shown in figure 9. This clearly shows four components: a sharp Bragg peak with a width of 0.0011(1) Å^{-1}, a broad peak with a width of 0.0052(1) Å^{-1}, one pair of satellites with positions ±0.0076(1) Å^{-1} and width of 0.0046(1) Å^{-1} and another pair of satellites with positions ±0.0179(3) Å^{-1} and width of ±0.0121(10) Å^{-1}. These results show that the positions of the outer satellites are proportional to the wavevector transfer suggesting that they arise from tilts in the layer. The inner satellite at the (006) Bragg reflection is not observed near (004), possibly because it cannot be distinguished from the

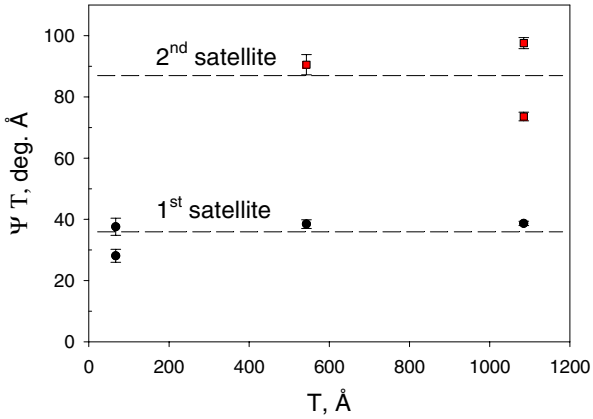

Figure 10. The positions of the first and second satellites plotted against film thickness T as measured in transverse scans, figures 9, 10, and calculated from dislocation theory (dotted lines).

broad central component. Near the (002) Bragg reflection the broad central component is wider than at the (004) and (006) Bragg reflections, possibly because it includes scattering from the outer satellites that could not be separately resolved near (002). In conclusion, the scattering is consistent with tilting but with sufficient wavevector-independent broadening to smooth out the structure at small wavevector transfers.

The scattering observed from layer 3841 is shown in figures 8 and 9 and qualitatively looks similar to that for layer 3468 but shows less distinct structure. The scattering observed near the (006) Bragg reflection, figure 9, clearly contains four components: a narrow peak, a broad peak centred at $q_x = 0$ with a width of 0.005(4) Å^{-1}, satellite peaks centred at $\pm 0.0038(5)$ Å^{-1} with a width of 0.005(1) Å^{-1} and satellite peaks centred at $\pm 0.0097(8)$ Å^{-1} with a width of 0.0065(10) Å^{-1}. The scattering observed near (004), figure 8, clearly shows two components and on detailed analysis three components: there is a narrow and a broad peak centred at $q_x = 0$ with a width of 0.0008(1) and 0.0036(1) Å^{-1} and then satellite peaks centred on $\pm 0.0056(4)$ Å^{-1} with width of 0.0080(5) Å^{-1}. Finally, near the (002) Bragg reflection the scattering can be described by two components centred on $q_x = 0$ with widths of 0.000 41(5) and 0.0060(3) Å^{-1}.

In conclusion, the scattering from the three thinnest layers is complex and shows evidence for both tilting and correlated fluctuations in the positions of the planes. It is however clear from figures 8 and 9 that the overall width of the scattering decreases with increasing layer thickness. This is shown, at least approximately, for the satellite positions in figure 10 where we show the tilt angles $\Psi = \arctan(q_x/q_z)$ corresponding to the positions of the satellites (q_x, q_z) multiplied by T, the layer thickness. As the peaks are broad and overlapping, the parameters are somewhat uncertain, but the results, figure 10, do indicate that the angles are at least approximately inversely proportional to the layer thickness, T. The average values of ΨT are 36(4)° Å for the first and 87(10)° Å for the second satellite reflections.

Further information about the scattering was obtained from scans of the scattering wavevector along the q_z-direction while the q_x-component was fixed such that the scan passes through one of the satellite peaks. The results obtained for the 543 Å layer, 3468, gave a coherence length in the z-direction of 501 Å which is comparable to the layer thickness. This implies that the satellites arise from tilts that propagate through the whole thickness of the layer.

The scattering from the three thickest layers, 3885, 3873 and 3863, could be described by a single-Gaussian profile as shown in figures 8(d) and 9(d). The width of the Bragg reflections

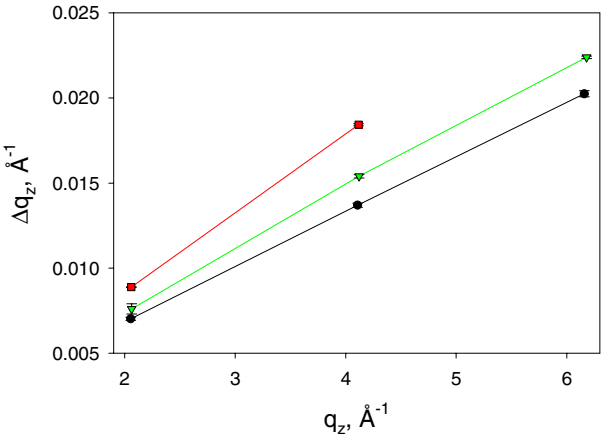

Figure 11. Measured widths of the Bragg reflections in transverse scans of the wavevector as a function of q_z for the 1370 Å (●), 3000 Å (▼) and 2700 Å (■) samples.

increases proportionally to the wavevector transfer L and, for example, for the 1370 Å layer (sample 3885) is 0.0070(1) for the (002) Bragg peak, 0.0137(1) for the (004) and 0.0203(2) for the (006) reflection as shown in figure 11. This behaviour is characteristic of a mosaic crystal and the mosaic spreads are (FWHM) 0.191(3)°, 0.257(2)° and 0.212(3)° for layers 3885, 3873 and 3863 respectively.

In order to examine whether the scattering is similar when the layer is in tension instead of compression, one layer of InAs grown on a GaSb substrate was also examined. The Pendellösung fringes were in this case not clearly defined and unfortunately the width of the (002) Bragg reflection was also poorly defined as well as the width of the (002) Bragg reflection, so the extrapolation method was inaccurate. This was at least in part because the GaSb substrate was not as perfect as the InAs substrates. As a result, the thickness was obtained as 720(200) Å. Transverse scans through the (002), (004) and (006) InAs Bragg reflections are shown in figure 12. The results are qualitatively similar to those obtained for a similar thickness of GaSb layer. There is a component centred on $q_x = 0$ and near (002) this clearly consists of two parts: a narrow component with a correlation length of about 20 000 Å and a broader component with a correlation length of about 1200 Å. Near the (004) and (006) Bragg reflections this component is narrower corresponding to a correlation length of about 2400 Å. However, in addition to the scattering centred at $q_x = 0$, satellites are observed near (004) and (006) reflections. Around the (006) InAs Bragg peak, satellites are observed with $q_x = \pm 0.0032(5)$ Å^{-1} and with $q_x = \pm 0.0074(4)$ Å^{-1}. Near the (004) reflection, only one satellite is clearly visible with $q_x = \pm 0.0046(1)$ Å^{-1}. The values of ΨT for the satellites of InAs are 21(7)° Å for the first satellite and 48(15)° Å for the second satellite. The FWHM of the satellites increases only slightly with increasing wavevector: the satellites near the (004) InAs reflection have $\Delta q_x = 0.0048(1)$ Å^{-1} and the ones at (006) have $\Delta q_x = 0.0022(1)$ Å^{-1} and $\Delta q_x = 0.0055(1)$ Å for the first and second satellites respectively. The width of the outermost satellites corresponds to a correlation range of about 1300 Å. There is much similarity between the results for InAs and GaSb layers with the data for InAs lying intermediate between those for GaSb samples 3468 and 3841. The positions of the satellites ΨT differ by a factor of 1.75 but this is possibly due to a large error in the thickness of the layer. Good agreement would be obtained if the thickness was 1260 Å.

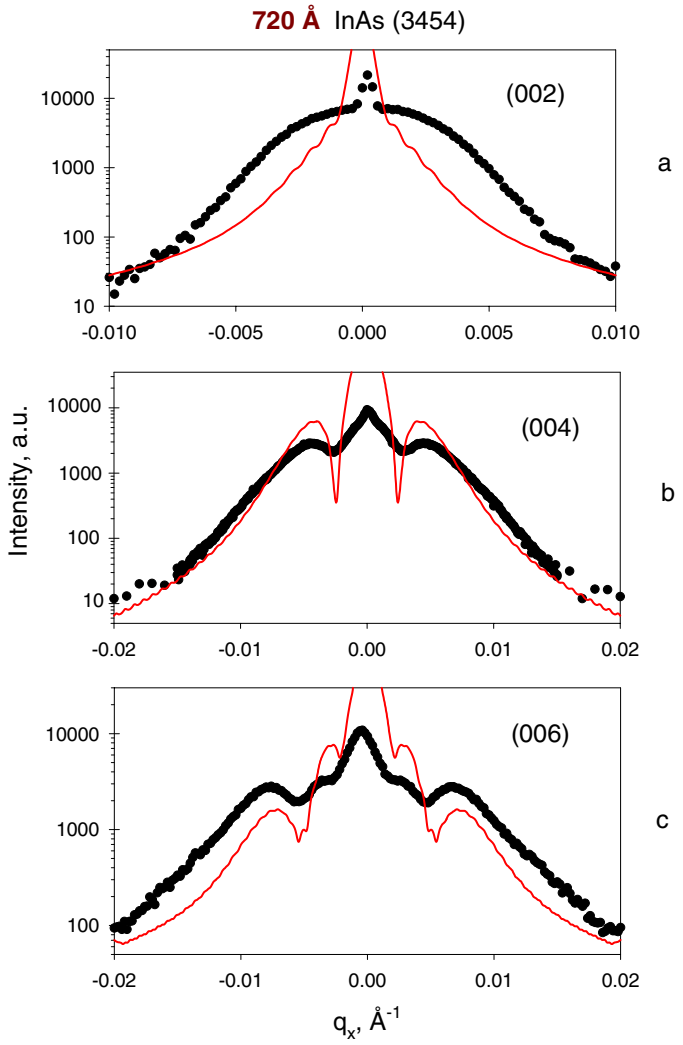

Figure 12. X-ray scattering observed from an InAs thin film grown on a GaSb substrate measured with transverse scans through the (002), (004) and (006) Bragg reflections. The solid curves show calculations of the scattering from isolated 60° dislocations performed with the thickness twice as large as that given in table 1.

5. Scattering from dislocations

Many properties of the scattering described above can be understood in terms of the x-ray diffraction from misfit dislocations [4]. The scattering is clearly different for the three thinner GaSb layers to that for the three thicker layers, so there is a transition for a thickness T_c' of about 1250(100) Å. In this section we shall show that the scattering from two of the thinner layers is consistent with the scattering to be expected for a low density of dislocations in the layer, whereas the results for the thicker layers are consistent with the scattering to be expected if there is a large density of dislocations.

According to the theory [4], at small densities of isolated dislocations ($\rho T \lesssim 1$, where ρ is the linear dislocation density), the scattered intensity contains a narrow component, which

comes from practically undistorted regions between the dislocations. The diffuse intensity arises from the strongly distorted regions around the dislocations. An important prediction of the theory is the appearance of satellite peaks when the wavevector transfer is scanned transversely if the misfit dislocations are 60° dislocations. The displacements of the atoms around a dislocation can be calculated using elasticity theory for a continuum and the results are listed in appendix B of [4]. The scattering to be expected from an isolated 60° dislocation has been calculated using this formalism. The choice of 60° dislocations was firstly because the measurements showed that the defects propagate through the whole layer and this occurs for 60° dislocations but not for 90° dislocations [14]. Secondly the shape of the diffuse scattering predicted by the continuum theory is the same for all thicknesses of the layers provided that the wavevector difference from the Bragg reflections is scaled with the layer thickness as indicated by the results shown in figure 10. The calculations give the product of the peak positions and the thickness, ΨT, as 43(2)° Å for the first satellite and 94(9)° Å for the second satellite, which are in good agreement with the results shown in figure 10, namely 36(4)° Å for the first satellite and 87(10)° Å for the second satellite.

More precisely, the continuum theory has been used to calculate the scattering for layers with different numbers of atomic planes. The calculations used the Poisson's ratio of GaSb and the appropriate lattice parameters and the results are shown in figures 8, 9 and 12 where they are compared with the observed scattering. The calculated results were scaled to the experimental measurements of the diffuse scattering and for the GaSb layers the thickness was increased by a factor of 1.13 so that the positions of the peaks were in good agreement with the observed peaks. No attempt was made to reproduce the intensity or shape of the Bragg-like central component. The agreement between the theory and the experimental results is excellent for the diffuse scattering for the GaSb layer, 3468, with a thicknesses of 543 Å, figures 8(b) and 9(b). There are larger discrepancies for the thinnest layer. This is possibly because of the failure of the continuum approximation to describe a layer of only 12 unit cells, but also possibly because the diffuse scattering may arise from fluctuations in the thickness of the thin film or from interface defects. The satellite peaks in the diffuse scattering are broader for layers 3841 and 3454 than in the calculations. Possibly this is because the model of independent isolated dislocations is inadequate.

For the thicker layers, 3885, 3873 and 3863, there is a single peak in the scattering that is well described by a Gaussian and its width in both q_x and q_z increases almost linearly with increasing wavevector transfer. The scattering does not show the satellite peaks or Pendellösung fringes that are observed for the thinner samples. The lack of thickness fringes is an indication of relaxation in the layer arising most likely from an increased density of mismatch dislocations [15]. These results are consistent with the theory of the scattering from misfit dislocations given by Kaganer *et al* [4] for high dislocation densities $\rho T \gg 1$. The FWHM in the q_x- and q_z-directions, Δq_x and Δq_z, depend on the type of dislocation. According to the theory, the peak aspect ratio $\Delta q_x/\Delta q_z$ is about 0.64 for edge dislocations and $\sqrt{6/11}\frac{\nu}{1-\nu} \approx 0.34$ for 60° dislocations, where ν is the Poisson ratio which is 0.313 for GaSb. Furthermore, the widths at the (004) Bragg reflection are related to the density of 60° dislocations, ρ, to an accuracy of 10% by [4]

$$\rho = \left(\frac{\Delta q_x}{21.3}\right)^2 T; \qquad \rho = \left(\frac{\Delta q_z}{6.2}\right)^2 T. \tag{4}$$

Our results give the ratios $\Delta q_x/\Delta q_z = 0.31(2), 0.27(3)$ and $0.31(3)$ for the samples 3885 (1370 Å), 3873 (2700 Å) and 3863 (3000 Å) respectively and confirm that networks of 60° dislocations are responsible for the peak broadening. The dislocation densities and hence the mean separation between the dislocations, D, were obtained and the densities are shown in

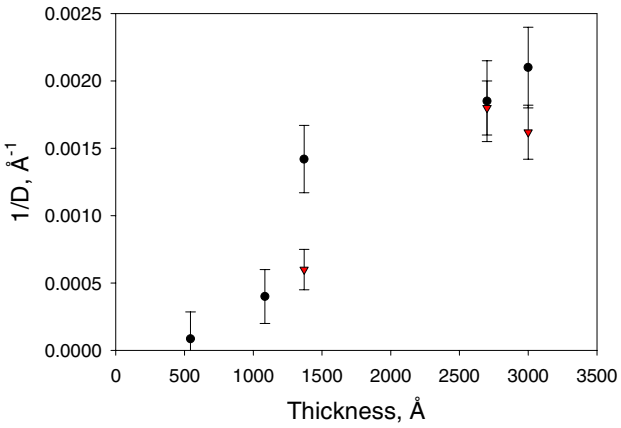

Figure 13. The density of dislocations versus the layer thickness calculated from the lattice parameters (●) and from the widths of the Bragg peaks (▼).

figure 13. For the three thick samples, $\rho T = T/D \approx 0.83$, 4.7 and 4.8 for samples 3885, 3873 and 3863 respectively. It is possibly surprising that the theory for $\rho T \gg 1$ gives such a satisfactory account of these results.

The average dislocation spacing can also be calculated from the Burgers vector and the lattice mismatch [5]. 60° dislocations have an edge component of the Burgers vector in [110] direction $b_{eff} = a \cos 60°/\sqrt{2}$ and an average separation distance between the dislocations D can be found from

$$D = \frac{b_{eff}}{f^{\parallel}} \tag{5}$$

where $f^{\parallel} = \Delta a/a$ is the measured in-plane lattice mismatch and Δa is shown in figure 6. These results for the dislocation density are also shown in figure 13. The agreement between the two calculations for ρ is clearly very satisfactory for the two thickest layers. For the layers close to T_c' it is probably unreasonable to expect the large-density theory to give reasonable results. The results are however consistent with the limits on the theory [4] that for the thinnest layers $D > T$ while for the thicker layers $D < T$.

The critical thickness for the onset of 60° dislocations can be calculated from the theory of Matthews and Blakeslee and others as reviewed and summarized, for example, in [16]. The result is $T_c = 204$ Å. This is based on the continuum theory with the dislocation core parameter $\alpha = 4$. The form of the expression makes it however very unlikely that the critical thickness can be in error by more than a factor of 2. The critical thickness is therefore significantly lower than the thickness T_c' determined as the onset of a dislocation network and significant lattice parameter relaxation. The scattering from thin layers of GaSb indicated a very low density of dislocations for all thicknesses of layers below 1000 Å. For example, for the layer 3468 with the thickness $T > 2T_c$, the distance between the dislocations is about 10^4 Å, figure 13, and is too big to produce any significant relaxation or strain field. The measured diffraction patterns exhibit Pendellösung fringes, figure 4, and little indication of uniform or non-uniform strains, figures 5(a), 6 and 7. Nevertheless we do clearly observe diffuse scattering from 60° dislocations from samples 3468, 3841 and 3454. These results suggest that the calculated critical thickness is correct at about 204 Å but that a dislocation network is only produced for thicknesses above T_c' about 1250 Å. We note that T_c' is close to the thickness at which the equilibrium spacing between the dislocations becomes approximately the same as the

layer thickness. This behaviour may arise if it is not possible to nucleate the dislocations as discussed in the review by Jain *et al* [16] for thicknesses between T_c and T_c'. Our results could then be understood if above the critical thickness only a few dislocations were nucleated on steps or other defects and significant numbers of dislocations were produced only above the thickness T_c'.

6. Summary and discussion

The paper reports on the x-ray scattering from GaSb epilayers grown on InAs substrates with a range of thicknesses between 67 and 3000 Å. These thicknesses span the critical thickness above which the in-plane lattice parameters of the substrate and layers differ. The paper reports that the x-ray scattering from the layers changes markedly as the thickness is increased through the critical thickness. Below a critical thickness T_c' the longitudinal scans through the Bragg reflections have the same widths and show Pendellösung fringes, whereas above this thickness there are no Pendellösung fringes and the widths of the Bragg peaks increase with increasing Bragg index. This latter result inhibits an accurate determination of the layer thicknesses with x-ray techniques. The transverse scans through the Bragg peaks also differ. Below the critical thickness there is a sharp component with a width comparable to that of the substrate, the in-plane lattice parameter is not significantly different from that of the substrate and there is complex diffuse scattering that changes shape as the index of the Bragg scattering increases. Above the critical thickness the results are characteristic of mosaic crystals with a Gaussian distribution of domains and there is a marked difference between the in-plane lattice parameter of the layer and that of the substrate. The change between the two regimes occurs when the thickness is about 1250 Å and is accompanied by a rapid change of most structural properties of the layers. The relaxation parameter defined as $R = \Delta a/\Delta a_{bulk}$ increases dramatically to 50% for a 1370 Å layer and then slowly to 72% for a 3000 Å sample leaving a residual strain of approximately 0.17%. That means that even the thick layers of GaSb are not fully relaxed and this is consistent with the prediction of the theory [17]. We have shown that this scattering can be understood as that from the layers with the distance between the dislocations, D, much bigger than the thickness, T, for thinner layers and $D \ll T$ for the thicker layers.

This critical thickness $T_c' = 1250(100)$ Å is significantly higher than the theoretical value of the critical thickness for the onset of dislocations $T_c = 204$ Å. An unexpected feature of our results is that the scattering clearly shows the presence of isolated 60° dislocations for layers thicker than T_c but considerably thinner than T_c'. This suggests that for these thicknesses it is difficult to nucleate the equilibrium number of dislocations. For thicknesses larger than T_c' there is a rapid increase in the dislocation density because the dislocations can be spontaneously nucleated. The dislocation densities deduced from the lattice mismatch and from the width of the Bragg reflections are consistent. These dislocations relax the strain and propagate through the thickness of the layer. The top of the layer is then rough which prevents the observation of the thickness fringes in the longitudinal scans. For layers thinner than T_c' there are only very few dislocations, possibly nucleated on defects or steps of the substrate, and these only relax a very small amount of the strain.

We have also made measurements on one layer of InAs on a GaSb substrate. The results are qualitatively similar to those for the GaSb layers of the same thickness.

In conclusion, these results have shown that x-ray scattering is an extremely sensitive non-destructive tool for probing changes in the dislocation structure of epitaxial layers; measurements of the scattering around several Bragg reflections enable many aspects of the structure to be determined unambiguously. We have shown that it enables us to determine the strain, the variation of the strain through the layer, the nature of the dislocation network,

the dislocation types and the critical thicknesses for the onset of dislocations and for the spontaneous nucleation of dislocations. We consider that these results show that high-resolution x-ray measurements can provide much more information about the structure of thin films than has usually been obtained and hope that the full potential of the x-ray scattering will be exploited in the future.

Acknowledgments

The work was funded by the UK Engineering and Physical Sciences Research Council (EPSRC). This work was performed on the EPSRC-funded XMaS beamline at the ESRF. We are grateful to the beamline team for their invaluable assistance. We would like to thank Mark Bentall for assistance with the experiments.

References

[1] Beanland R, Dunstan D J and Goodhew P J 1996 *Adv. Phys.* **45** 87
[2] Jain S C, Willis J R and Bullough R 1990 *Adv. Phys.* **39** 127
[3] Bennett B R 1998 *Appl. Phys. Lett.* **73** 3736
[4] Kaganer V M, Köhler R, Schmidbauer M, Opitz R and Jenichen B 1997 *Phys. Rev.* B **55** 1793
[5] Booker G R *et al* 1997 *J. Cryst. Growth* **170** 777
[6] Langford J I 1978 *J. Appl. Crystallogr.* **11** 10
[7] Langford J I 1992 *National Institute of Standards and Technology Special Publication vol 846* (Washington, DC: National Institute of Standards and Technology) pp 110–25
[8] Kolpakov A V, Khapachev Y P, Kuznetsov G F and Kuzmin R N 1977 *Sov. Phys.–Crystallogr.* **22** 269
[9] Chukhovskii F N, Gabrielyan K T and Petrashen P V 1978 *Acta Crystallogr.* **34** 610
[10] Punegov V I 1990 *Sov. Phys.–Crystallogr.* **35** 336
[11] Lin W J, Hatton P D, Baudenbacher F and Santiso J 1998 *Appl. Phys. Lett.* **72** 2966
[12] Fewster P F 1992 *J. Appl. Crystallogr.* **25** 714
[13] Kidd P, Fewster P F and Andrew N L 1998 *J. Appl. Phys.* D **28** A133
[14] Babkevich A Y, Cowley R A, Mason N J and Stunault A 2000 *J. Phys.: Condens. Matter* **12** 4747
[15] Halliwell M A G 1997 *J. Cryst. Growth* **170** 47
[16] Jain S C, Harker A H and Cowley R A 1997 *Phil. Mag.* **75** 1461
[17] Gosling T J, Willis J R, Bullough R and Jain S C 1993 *Japan. J. Appl. Phys.* **73** 8297